Vol 13 No 6, June 2004
1009-1963/2004/13(06)/0905-08

Chinese Physics

© 2004 Chin. Phys. Soc.
and IOP Publishing Ltd

Chirping and spreading of ultrashort laser pulses in underdense plasmas*

Zhang Qiu-Ju(张秋菊), Sheng Zheng-Ming(盛政明), and Zhang Jie(张 杰)

Laboratory of Optical Physics, Institute of Physics, Chinese Academy of Sciences, Beijing 100080, *China*

(Received 16 May 2003; revised manuscript received 2 February 2004)

A linear theory on the propagation of ultrashort pulses including only a few cycles in underdense plasmas is presented. It is shown that the dispersion in plasmas causes severe distortions in the pulse shape, including pulse chirping and spreading. The analytical calculations coincide very well with those obtained by particle-in-cell (PIC) simulations. The upper limit of the peak amplitude of the pulses, above which the linear theory breaks down due to the setting in of nonlinear effects of both the relativistic electron-mass increase and ponderomotive force, is also examined by PIC simulations. At certain high amplitudes, it is found that the ultrashort laser pulses can propagate like solitons.

Keywords: propagation, ultrashort laser pulse, plasma
PACC: 5240D, 5255D, 5265

1. Introduction

Since ultrashort laser pulses generated based upon the mode-locking and chirped pulse amplification (CPA) technology have found wide applications in different scientific disciplines, the ultrafast science has emerged.[1,2] Recent development of ultrafast optics has allowed the generation of ultrashort laser pulses comprising merely a few oscillation cycles.[3−6] Obviously, one of the fundamental problems with such ultrashort laser pulses is the propagation properties in a variety of optical materials with different nonlinearities and dispersion. The interaction of ultrashort laser pulses with plasmas is fundamentally interesting in laser plasma,[7−13] and it is also related to various applications in plasma wave excitation and particle acceleration.[1] Up to now, most of the studies on the ultrashort pulse laser interaction with plasmas concentrate on the cases when the pulse intensity is very high, such as over 10^{17} W/cm^2, at which various nonlinearities set in, and its duration is longer than a few tens of laser cycles. Little attention has been paid to the propagation of ultrashort pulse with only a few cycles in plasma.

In this paper, we present a linear analysis on the propagation of an ultrashort laser pulse with only a few cycles in an underdense plasma. This enables us to isolate the nonlinearities and see clearly the propagation features of such a pulse only due to the plasma dispersion. This helps us to understand the more complicated coupling between the nonlinearities and plasma dispersion when the pulse is at a high intensity. To our knowledge, this problem has not yet been tackled sufficiently. To obtain the evolution of a laser pulse, generally one can employ either Fourier analysis [14] or a Taylor series expansion of the spectrum about the carrier frequency.[15] Here, we calculate the evolution of an ultrashort pulse with the Fourier analysis method. We present a general theory first, then apply it to two specific profiles of ultrashort pulses comprising only three oscillating cycles. Our calculations show a severe distortion in the pulse shape as it propagates: the pulse envelope spreads out and the pulse oscillation with time becomes inhomogeneous throughout the pulse duration, i.e. pulse chirps arise. The results agree with those obtained by the particle-in-cell (PIC) simulations, showing that the numerical Fourier analysis can give a correct description of the dispersive pulse dynamics. Because of the very abundant spectrum component of the ultrashort pulses, the chirping and spreading are more prominent than those when the duration of pulse is longer than a few tens of laser cycles.

With the increase of laser pulse amplitude, the

*Project supported by the National Natural Science Foundation of China (Grant Nos 10105014, 19825110 and 10075075), the 'Hundred Talents Programme' of the Chinese Academy of Sciences, and the National High-Technology Inertial Confinement Fusion Foundation of China.

nonlinearity effects appear due to the relativistic increase of the electron mass and the action of the ponderomotive force. The dispersion effects can make the laser pulse spread, while the nonlinearity effects can compress it. At certain pulse amplitude, the coupling of these effects lead to relativistic electromagnetic soliton generation. Numerical examples of soliton-like pulse formation for pulses at a few cycles are also demonstrated in this paper.

2. Propagation of plane-waves in homogeneous and inhomogeneous plasmas

To study the propagation of an ultrashort laser pulse in a plasma, one needs to start with the propagation of an infinite plane light wave in the plasma. Assuming that there is no absorption in the plasma, the equation for the electric field component of the light wave with frequency ω in the plasma is given by [16,17]

$$\frac{\mathrm{d}^2E}{\mathrm{d}z^2}+\frac{\omega^2}{c^2}\varepsilon E=0, \tag{1}$$

where E is perpendicular to the propagation z-axis for either linear or circular polarization, $\varepsilon(\omega)=1-\omega_{\mathrm{p}}^2/\omega^2$, $\omega_{\mathrm{p}}^2=4\pi n(z)e^2/m$, with $n(z)$ being the initial electron density profile as a function of the z-coordinate.

In the case that the plasma density is homogeneous as shown in Fig.1(a), one can find the solution for Eq.(1) in different regions, labelled by a, b, and c. Assuming that the light wave propagates from left to right, one obtains

$$E_a=\mathrm{e}^{\mathrm{i}kz}+A\mathrm{e}^{-\mathrm{i}kz} \qquad (z\le 0), \tag{2}$$

$$E_b=B_1\mathrm{e}^{\mathrm{i}k_1z}+A_1\mathrm{e}^{-\mathrm{i}k_1z} \qquad (0\le z\le L), \tag{3}$$

$$E_c=B_2\mathrm{e}^{\mathrm{i}kz} \qquad (L\le z), \tag{4}$$

where $k=\omega/c$ is the wavenumber of the plane wave in vacuum, $k_1=\dfrac{\omega}{c}\sqrt{\varepsilon(\omega)}$ is the counterpart in plasmas and L is the length of the plasma slab. By utilizing the boundary conditions that E and $\mathrm{d}E/\mathrm{d}z$ continue at the vacuum–plasma boundary,[17] we obtain the coefficients

$$A=r_1r_2\left[1-\exp(\mathrm{i}\psi_1)\right]/\left[r_1^2-r_2^2\exp(\mathrm{i}\psi_1)\right],$$

$$A_1=-2r_2/\left[r_1^2-r_2^2\exp(\mathrm{i}\psi_1)\right],$$

$$B_1=2r_1/\left[r_1^2-r_2^2\exp(\mathrm{i}\psi_1)\right],$$

$$B_2=4\sqrt{\varepsilon(\omega)}\exp[\mathrm{i}(\psi_1/2-\mathrm{i}L\omega/c)]/\left[r_1^2-r_2^2\exp(\mathrm{i}\psi_1)\right],$$

where $r_1=1+\sqrt{\varepsilon}$, $r_2=1-\sqrt{\varepsilon}$ and $\psi_1=2L\sqrt{\varepsilon(\omega)}\omega/c$.

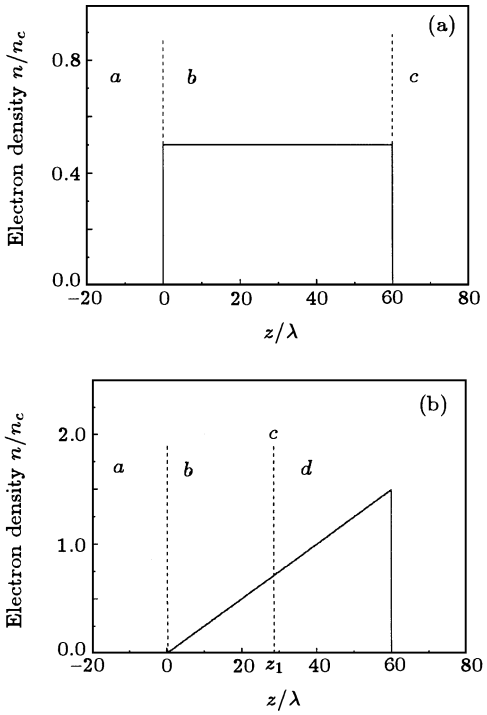


Fig.1. The electron density profile, with $n_c=m\omega_0^2/4\pi\mathrm{e}^2$ being the critical density for a carrier frequency ω_0. z is the spatial coordinate in wavelength $2\pi c/\omega_0$. (a) A homogeneous plasma slab with density $n=0.5n_c$. (b) The linear density profile.

When the plasma is inhomogeneous, the solution is generally more complicated. For the simplest case when the plasma is of a linear density profile as shown in Fig.1(b), the Airy function is the exact solution of the standing light wave in the plasma. However, the right- and left-going waves are combined in this function. When the density scale-length is much longer than a laser wavelength in vacuum, one can use the Wentzel–Krammer–Brillouin method to find the left- and right-going wave separately. We can divide the whole zone into four parts, labelled as a, b, c, and d; then the solution for Eq.(1) is given by

$$E_a=\mathrm{e}^{\mathrm{i}kz}+A\mathrm{e}^{-\mathrm{i}kz} \qquad (z\le 0), \tag{5}$$

$$E_b=\frac{A_1}{\varepsilon^{1/4}}\exp\left(\mathrm{i}\frac{\omega}{c}\int_0^z\sqrt{\varepsilon(z')}\mathrm{d}z'\right)+\frac{B_1}{\varepsilon^{1/4}}\exp\left(-\mathrm{i}\frac{\omega}{c}\int_0^z\sqrt{\varepsilon(z')}\mathrm{d}z'\right) \qquad (0\le z<z_1), \tag{6}$$

$$E_c=A_2A_i(\zeta)(z\approx z_1), \tag{7}$$

$$E_d=A_3\exp\left(-\frac{\omega}{c}\int_{z_1}^z\sqrt{\varepsilon(z')}\mathrm{d}z'\right) \qquad (z_1<z), \tag{8}$$

where $\zeta=\left(\dfrac{\omega^2}{c^2z_1}\right)^{1/3}(z_1-z)$, z_1 being the critical interface for the plane wave with frequency ω. By utilizing the boundary conditions at $z=0$ and around

z_1, we can obtain all the coefficients in the above expressions,

$$A = 2A_{\rm m}\cos(\psi_2) - 1, \tag{9}$$

$$A_1 = A_{\rm m}\exp(\mathrm{i}\psi_2), \tag{10}$$

$$B_1 = A_{\rm m}\exp(-\mathrm{i}\psi_2), \tag{11}$$

where

$$\psi_2 = \frac{\pi}{4} - \frac{2}{3}\frac{\omega}{c}z_1,$$

$$A_{\rm m} = \frac{\cos(\psi_2) - \mathrm{i}\left[\sin(\psi_2) - (4kz_1)^{-1}\cos(\psi_2)\right]}{\cos^2(\psi_2) + \left[\sin(\psi_2) - (4kz_1)^{-1}\cos(\psi_2)\right]^2}.$$

For an incident light pulse with a finite duration, $E(0,t)(0 \le t \le T)$ on the plane z=0, its frequency spectrum is given by $g(\omega) = \int_0^T E(t,0)\mathrm{e}^{-\mathrm{i}\omega t}\mathrm{d}t$. Then the solution for the laser pulse in vacuum or in the plasma at given time t is simply the integral over the frequency space,

$$E(z,t) = \frac{1}{2\pi}\int_{-\infty}^{\infty} g(\omega)R(z,\omega)\mathrm{e}^{-\mathrm{i}\phi(z,\omega)+\mathrm{i}\omega t}\mathrm{d}\omega, \tag{12}$$

where the $R(z,\omega)$ and $\phi(z,\omega)$ are respectively the amplitude and the phase of the corresponding plane wave solution $E(z,\omega)$ with frequency ω obtained before. By Eq.(12), the temporal and spatial evolution of the ultrashort laser pulse in plasma can be determined.

3. Propagation of ultrashort laser pulses in plasmas

Generally, Eq.(12) cannot be integrated analytically, even for the simplest case of pulse propagating in a homogeneous plasma. Thus one has to integrate Eq.(12) numerically. In the following, we consider two specific pulse profiles, i.e. the rectangular profile and the sine square profile.

3.1. Propagation of ultrashort pulses with a rectangular profile

For a rectangular pulse as shown in Fig.2(a), the initial pulse field at the plane z=0 is given by $E(0,t) = E_0\sin(\omega_0 t)$ for $0 \le t \le T$, where $T = 2p\pi/\omega_0$ and p is an integer. Then the Fourier transform of the input pulse field $E(0,t)$ can be obtained as

$$g(\omega) = E_0\frac{(-1)^p}{2\mathrm{i}}T\mathrm{e}^{-\mathrm{i}\omega\frac{T}{2}} \times \left[\frac{\sin\frac{T}{2}(\omega_0-\omega)}{\frac{T}{2}(\omega_0-\omega)} - \frac{\sin\frac{T}{2}(\omega_0+\omega)}{\frac{T}{2}(\omega_0+\omega)}\right]. \tag{13}$$

Substituting Eqs.(2)–(6) and (13) into Eq.(12), we can obtain the propagating and reflected pulses inside and outside the plasma. We set $p = 3$ in the following calculation.

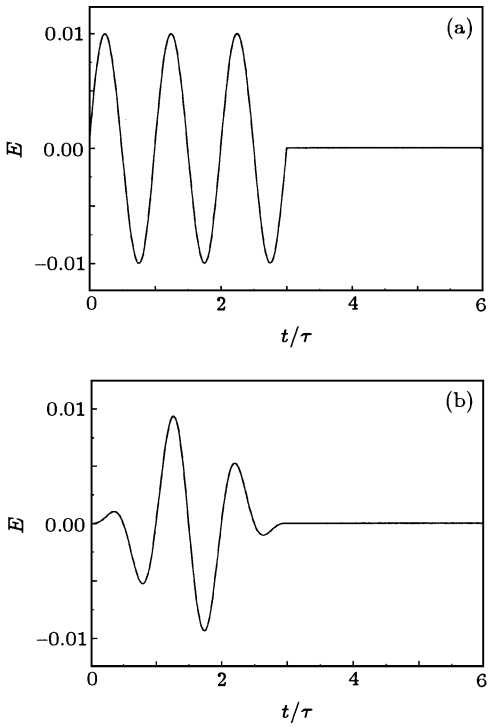


Fig.2. The input pulse with three laser cycles and E_0=0.010. (a) The rectangular pulse $E(0,t) = E_0\sin(\omega_0 t)$. (b) The $\sin^2$ pulse $E(0,t) = E_0\sin^2(\pi t/T)\sin(\omega_0 t)$.

Firstly, we calculate the pulse in a homogeneous plasma as in Fig.1(a), where we set the plasma length $L = 60\lambda$. Figure 3(a) shows the typical result of the pulse profile after propagating a few tens of laser wavelengths inside the plasma with a density of $0.5n_c$ obtained by numerical integration of Eq.(12). It shows that the shape of the propagating pulse is completely distorted from the initial rectangular shape owing to the plasma dispersion. On the one hand, the pulse is spreading out gradually as the pulse propagates forward. Finally the pulse length even extends to ten times of the initial one. Qualitatively, the pulse length follows a law[17] as given by $\Delta z(t) = [\Delta z_0^2 + (t\mathrm{d}^2\omega/\mathrm{d}k^2/\Delta z_0^2)^2]^{1/2} \approx (c/\varepsilon^{1/2}\omega_0)(n/n_c)(t/T)$, where $\Delta z_0 = cT$ is the initial pulse length, $\mathrm{d}^2\omega/\mathrm{d}k^2 = c^2\omega_{\rm p}^2/\omega^3$. On the other hand, because the initial pulse is only of a few cycles, it has a broad frequency spectrum. The components with high frequencies propagate at high group velocities. As a result, a frequency chirping phenomenon arises, with the leading front of the pulse oscillating at high frequency and the trailing edge of the pulse at low frequency, as shown in Fig.3(a). To check the validity of the numerical calculations, we have performed PIC simulations on the

same condition as in Fig.3(a) with the peak amplitude of $E_0 = 0.01$, where E_0 is normalized by $mc\omega_0/e$. The result of the PIC simulation is given in Fig.3(b) at the same time, which coincides with Fig.3(a) obviously. Figure 4 shows the laser pulse propagating out of the right plasma–vacuum boundary. The pulse shows a decaying long tail, which decays as $E(t) = (t - z/c)^{-1} \int_{-\infty}^{\infty} \partial F(\omega)/\partial\omega e^{i\omega(t-z/c)} d\omega \approx O(1/t)$ for $t \to \infty$, where $F(\omega) = (2\pi i)^{-1} B_2(\omega) g(\omega)$.

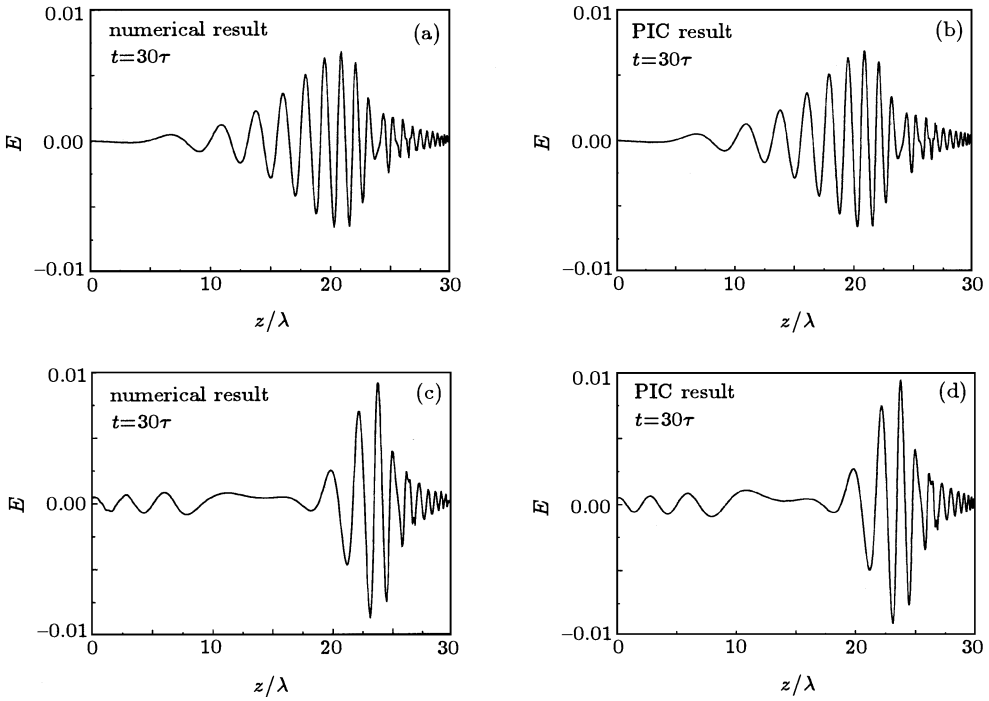


Fig.3. Snapshots of a rectangular pulse in the homogeneous plasma slab obtained numerically (a) and by the PIC simulation (b). The snapshot of the same pulse propagating in an inhomogeneous plasma obtained numerically and by the PIC simulations are given in (c) and (d), respectively.

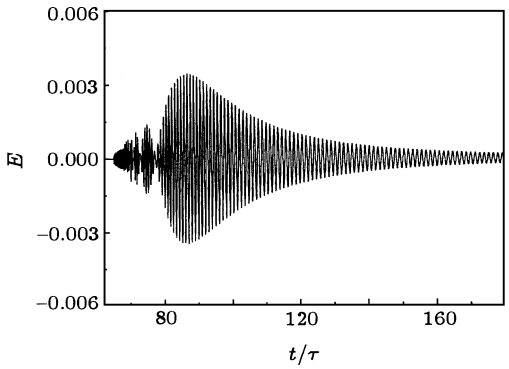


Fig.4. The transmitted pulse through the homogeneous plasma slab as a function of time when the input pulse is in the rectangular profile in three cycles.

Secondly, we calculate the propagation of the rectangular ultrashort laser pulse in an inhomogeneous plasma with a linear density profile as shown in Fig.1(b). A snapshot of the pulse in the plasma is shown in Fig.3(c). As in a homogeneous plasma, one cannot see obviously any character retained with its initial pulse profile after the pulse propagates a few tens of the laser wavelength in the plasma. Meanwhile, similar pulse chirping and spreading are found. However, the spreading does not develop as quickly as it does in homogeneous plasma. This is because the leading front of the pulse, which has a higher frequency, also sees a higher density than the trailing edge. As an estimate, one notes that the difference of the group velocities between the leading and trailing edges is

$$\Delta v_g = c[\sqrt{\varepsilon(z_l, \omega_l)} - \sqrt{\varepsilon(z_t, \omega_t)}],$$

where z_l and z_t are the positions of the leading and trailing edges of the pulse, and ω_l and ω_t are the local frequencies of the leading and trailing edges, respectively. Thus one finds approximately

$$\Delta z = \Delta v_g t \approx \frac{c}{\omega_0} \frac{n(z)}{n_c \varepsilon(z)^{1/2}} \frac{t}{T} \left(1 + \frac{ct}{2\varepsilon^{1/2}} \frac{1}{n_c} \frac{dn}{dz}\right)^{-1}.$$

This shows obviously that the spreading develops slowly in an inhomogeneous plasma when $dn/dz > 0$. Note that when the plasma density changes gradually as compared with the pulse length and when

$(ct/2\varepsilon^{1/2})(\mathrm{d}n/\mathrm{d}z)/n_c \gg 1$, the final pulse length appears independent of time.

3.2. Propagation of ultrashort pulses with a sin square profile

Here we consider the case when the initial pulse field at z=0 is given by

$$E(t,0) = E_0 \sin^2\left(\frac{\pi t}{T}\right)\sin(\omega_0 t) \qquad 0 \le t \le T, \quad (14)$$

where $\omega_0 T = 2p\pi/\omega_0$ with p being an integer. The Fourier transform of the input pulse $E(0,t)$ is

$$g(\omega) = E_0 \frac{(-1)^{p+1}}{2\mathrm{i}} T \mathrm{e}^{-\mathrm{i}\omega\frac{T}{2}}\left[-g_1(\omega) - \frac{g_2(\omega)}{2}\right], \quad (15)$$

where $g_1(\omega)$ and $g_2(\omega)$ are given by

$$g_1(\omega) = \left[\frac{\sin\frac{T}{2}(\omega_0-\omega)}{\frac{T}{2}(\omega_0-\omega)} - \frac{\sin\frac{T}{2}(\omega_0+\omega)}{\frac{T}{2}(\omega_0+\omega)}\right],$$

$$g_2(\omega) = \frac{\sin(\Omega_{\mathrm{p}}^- T)}{\Omega_{\mathrm{p}}^- T} - \frac{\sin(\Omega_{\mathrm{p}}^+ T)}{\Omega_{\mathrm{p}}^+ T} + \frac{\sin(\Omega_{\mathrm{m}}^- T)}{\Omega_{\mathrm{m}}^- T} - \frac{\sin(\Omega_{\mathrm{m}}^+ T)}{\Omega_{\mathrm{m}}^+ T},$$

with

$$\Omega_{\mathrm{p}}^{\pm} T = \frac{T}{2}\left[\omega_0\left(1+\frac{1}{p}\right) \pm \omega\right]$$

$$\Omega_{\mathrm{m}}^{\pm} T = \frac{T}{2}\left[\omega_0\left(1-\frac{1}{p}\right) \pm \omega\right].$$

Using Eqs.(2)–(6), (12) and (15), we can calculate the laser pulse propagating inside and outside the plasma. In the following, we also set $p = 3$, so that the incident pulse is as shown in Fig.2(b).

For the case when the plasma is homogeneous, a snapshot of the pulse inside the plasma is given in Fig.5(a). Spreading and chirping are observed in a way qualitatively similar to those when the pulse is in a rectangular profile. The corresponding PIC simulation result for the peak amplitude $E_0 = 0.01$ is given in Fig.5(b), which is again in agreement with the numerical calculation. In the case when the plasma is inhomogeneous with a linear density profile, snapshots of the pulse in the plasma obtained by Eq.(12) and PIC simulation are shown in Figs.5(c) and (d), respectively. As expected, the pulse spreads more slowly than that observed in a homogeneous plasma.

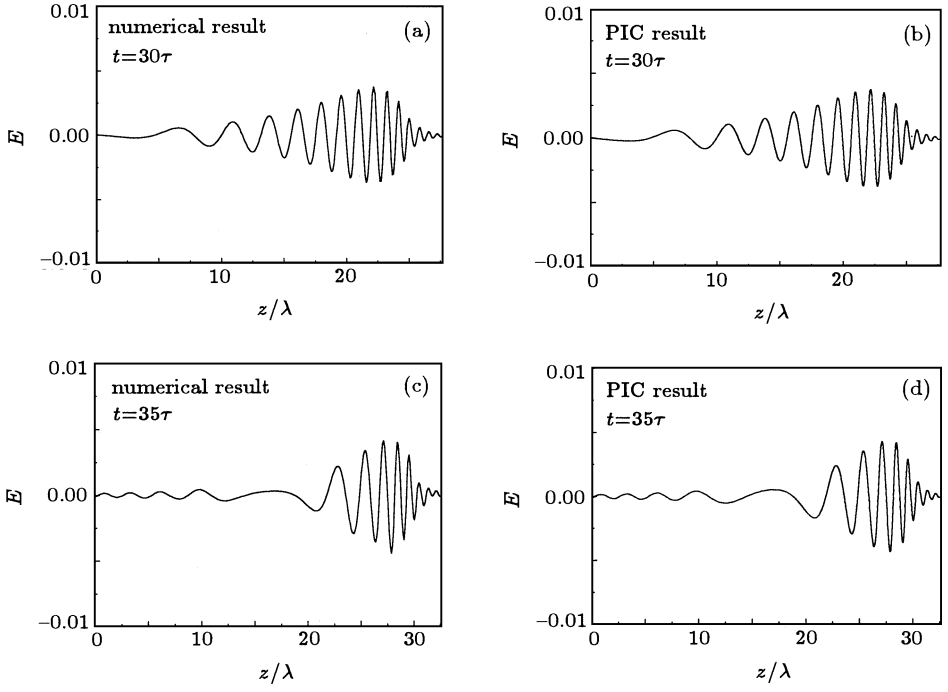


Fig.5. Snapshots of the input pulse $E(0,t) = E_0 \sin^2(\pi t/T)\sin(\omega_0 t)$ in the homogeneous plasma slab obtained numerically (a) and by the PIC simulation (b). Snapshots of the same pulse propagating in an inhomogeneous plasma obtained numerically and by PIC simulations are given in (c) and (d), respectively.

3.3. Upper limit of the pulse amplitude for the linear theory

The results given before are all in the linear regime, where there is no nonlinearity included. With the increase of the peak amplitude of the pulse, the linear calculation should break down finally. Here, with the help of PIC simulations we give an estimate of the upper limit of the pulse amplitude beyond which the linear theory breaks down. We use the three-cycle $\sin^2$

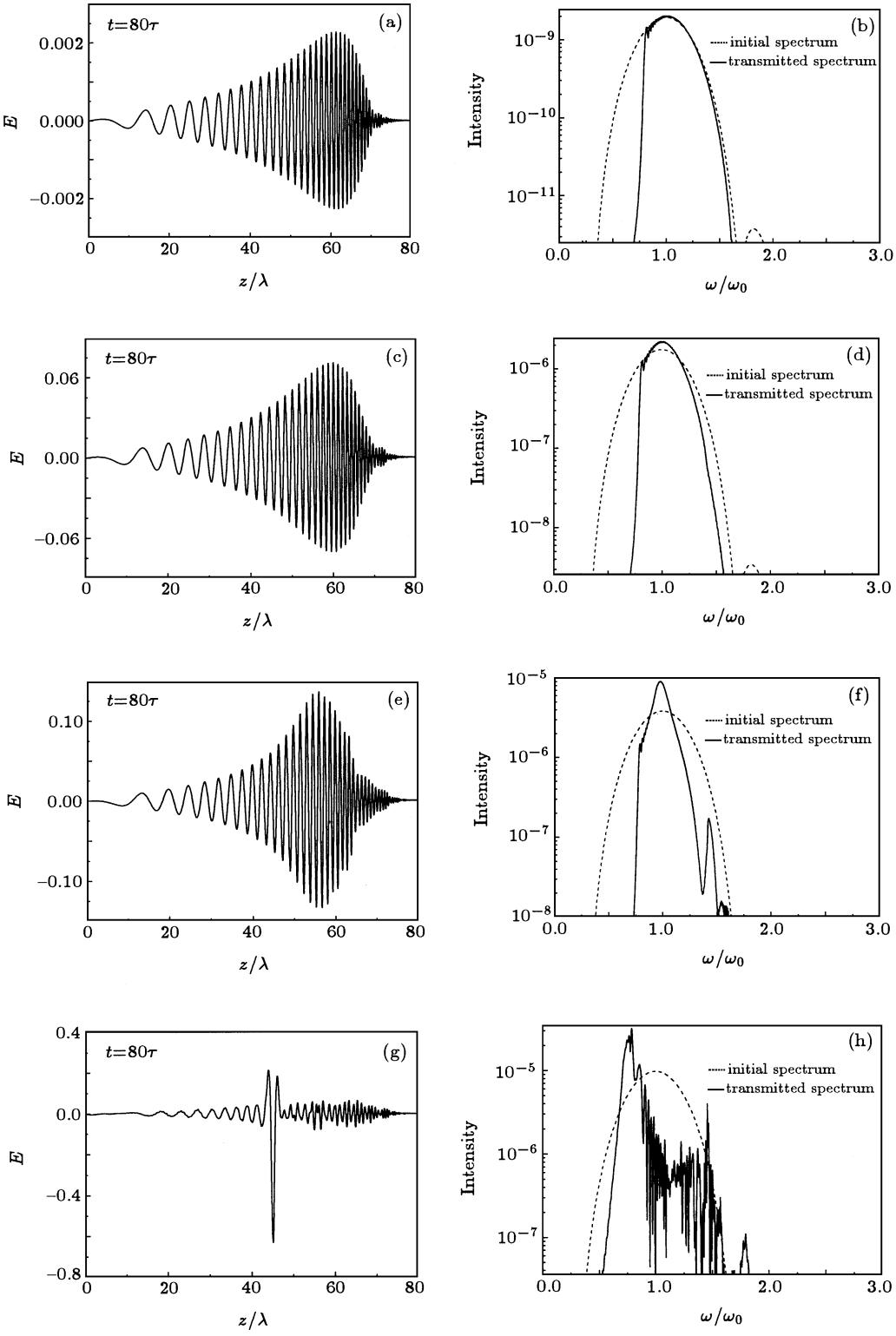


Fig.6. Snapshots of the pulse inside the homogeneous plasma slab (left column) and the corresponding frequency spectra of the pulse (right column) transmitted through the plasma slab for an input pulse $E_0 \sin^2(\pi t/T)\sin(\omega_0 t)$: (a) and (b), for $E_0 = 0.01$; (c) and (d), for $E_0 = 0.3$; (e) and (f), for $E_0 = 0.5$; (g) and (h), for $E_0 = 0.8$.

pulse in a homogeneous plasma as an example. Here the plasma occupies a length of 90λ, and its density is $n = 0.5n_c$. Figure 6 shows the snapshots of the pulses inside the plasma approaching the right plasma–vacuum boundary and the frequency spectra of the transmitted pulses through the plasma region at different peak amplitudes of the incident pulses. One notes that even in the linear regime, the spectrum of the transmitted pulse shown in Fig.6(b) is different from that of the incident pulse. The low-frequency part is reflected at the left vacuum–plasma boundary. The frequency cut appears around $\omega/\omega_0 = 0.7$, corresponding to the plasma density at $n = 0.5n_c$ used in the calculations. For $\omega/\omega_0 > 0.7$, the transmitted pulse spectrum is almost identical to that of the incident pulse, as expected.

When increasing the peak amplitude of the laser field to $E_0 = 0.3$, the nonlinear interaction begins to occur. Both the pulse profile and transmitted spectrum have slightly changed from the linear case, as shown in Figs.6(c) and (d). Thus this can be seen as the upper limit of the pulse peak amplitude, below which the linear analysis applies. Nonlinear effects set in when the peak amplitude of the laser pulse further increases. Figures 6(e) and (f) show the obvious change in the pulse profile and transmitted spectrum when $E_0 = 0.5$.

3.4. The generation of soliton

When the peak amplitude is increased further as in Figs.6(g) and (h), it is found that the pulse experiences a strong frequency down-shift, and the central frequency is close to the plasma frequency. The frequency down-shift is mainly due to the pulse self-phase-modulation as well as the cross-phase-modulation by the plasma density modulation driven by the ponderomotive force of the pulse.[18,19] When the nonlinearity effect is high enough to compensate the dispersive spreading, as shown in Fig.6(g), a soliton-like electromagnetic pulse forms. Figure 7 shows the temporal–spatial evolution of the ultrashort pulse for different pulse amplitudes. When the nonlinearity effect is very small as compared with the dispersion effect, the pulse spreads quickly and the pulse amplitude or energy decays rapidly in the whole space along with time, as shown in Fig.7(a). However, when the nonlinearity effect is approximately equal to the dispersion effect, a part of the pulse is converged to a soliton pulse, as shown in Fig.7(b). The soliton thus formed propagates quickly in the plasma slab with an approximately constant group velocity. We have also found that this propagating soliton is a peculiar phenomenon associated with the ultrashort pulse duration of only a few cycles. In earlier simulations with relatively long pulses, one observes only solitons trapped rather than propagating in the plasma.[20–22]

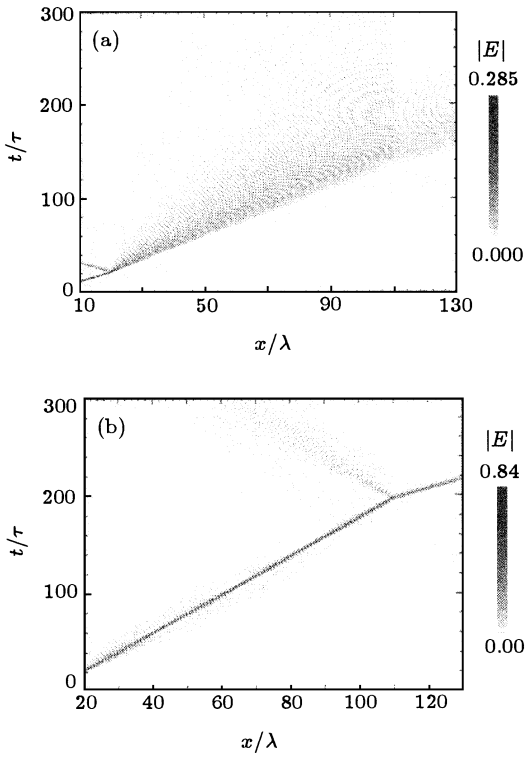


Fig.7. The temporal–spatial evolution of the laser pulse with the plasma slab $n = 0.7n_c$. (a) Dispersion effects for $E_0 = 0.3$. (b) Generation of soliton for $E_0 = 0.8$.

4. Summary

In summary, we have presented a linear analysis on the propagation of an ultrashort laser pulse in homogeneous and inhomogeneous plasmas. Significant pulse spreading and frequency chirping are found when the pulse is as short as a few laser cycles. After the pulse propagates a few tens of laser wavelength in the plasma, the pulse profile is reshaped completely. Because of the small energy contained in an ultrashort laser pulse with a few cycles, the linear theory can describe the pulse evolution in the plasma up to a peak amplitude around $E_0/(m\omega_0 c/e) \approx 0.3$, beyond which nonlinear effects begin to set in. In certain amplitudes, we observe that the ultrashort pulses propagate like a soliton, which results from the nonlinear effects compensated by the plasma dispersion.

References

[1] Mourou G, Barty C P and Perry M D 1998 *Phys. Today* **51** 22
Mourou G and Umstadter D 2002 *Scientific American* May 81
Umstadter D 2001 *Phys. Plasmas* **8** 1774

[2] Brabec T and Krausz F 2001 *Rev. Mod. Phys.* **72** 545

[3] Baltuška A, Wei Z Y, Pshenichnikov M S and Wiersma D A 1997 *Opt. Lett.* **22** 102

[4] Baltuška A, Wei Z Y, Pshenichnikov M S, Wiersma D A and Szipocs R 1997 *Appl. Phys.* B **74** 175

[5] Xu L, Tempea G, Poppe A, Lenzner M, Spielmann C, Krausz F, Stingl A and Ferencz K 2001 *Appl. Phys.* B **65** 151

[6] Wintner E 2002 *Laser Phys.* **12** 659

[7] Oghstun K E and Sherman G C 1990 *Phys. Rev.* A **41** 6090

[8] Le Blanca S P and Sauerbrey R 1994 *Opt. Commun.* **111** 297

[9] Christov I P 1995 *Opt. Commun.* **113** 530

[10] Nodlandand B and McKinstrie C J 1997 *Phys. Rev.* E **56** 7174

[11] Sheng Z M, Ma J X, Xu Z Z and Yu W 1993 *J. Opt. Soc. Am.* B **10** 122

[12] Sheng Z M, Sentoku Y, Mima K and Nishihara K 2000 *Phys. Rev.* E **62** 7258

[13] Tarasishin A V, Magnitskii S A and Zheltikov A M 2001 *Opt. Commun.* **193** 187

[14] Christov I P 1988 *IEEE J. Quant. Electron.* **24** 1548

[15] Anderson D, Askne J and Lisak M 1975 *Phys. Rev.* A **12** 1546

[16] Kruer W L 1988 *The Physics of Laser Plasma Interactions* (London: Addison-Wesley) p30

[17] Jackson J D 1998 *Classical Electrodynamics* 3rd ed (New York: Wiley) p296, 305

[18] Mima K, Jovanovic M S, Sentoku Y, Sheng Z M, Skoric M M and Sato T 2001 *Phys. Plasmas* **8** 2349

[19] Sheng Z M, Sentoku Y, Mima K, Nishihara K and Zhang J 2002 *Phys. Plasmas* **9** 3147

[20] Bulanov S V, Esirkepov T Z, Naumova N M, Pegoraro F and Vshivkov V A 1999 *Phys. Rev. Lett.* **82** 3440

[21] Naumova N M, Bulanov S V, Esirkepov T Z, Farina D, Nishihara K, Pegoraro F, Ruhl H and Sakharov A S 2001 *Phys. Rev. Lett.* **87** 185004

[22] Esirkepov T, Nishihara K, Bulanov S V and Pegoraro F 2002 *Phys. Rev. Lett.* **89** 275002